AD-A090 018 EPSILON LABS INC BEDFORD MA F/G 13/7
A MOLECULAR IDENTIFICATION DEVICE FOR INDIVIDUAL SUB-MICRON AER--ETC(U)
MAY 80 H A MIRANDA F19628-78-C-0168
UNCLASSIFIED AFGL-TR-80-0155 NL

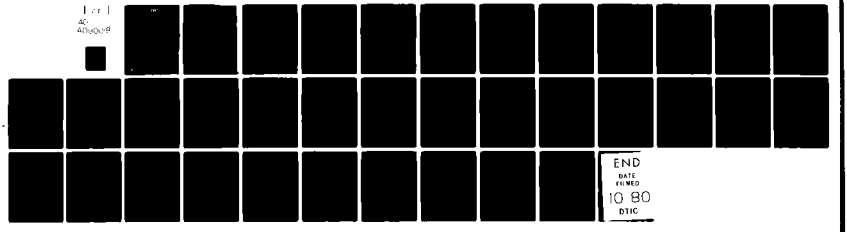

END
DATE FILMED
10 80
DTIC

LEVEL II

AFGL-TR-80-0155

A MOLECULAR IDENTIFICATION DEVICE FOR INDIVIDUAL SUB-MICRON AEROSOLS: FEASIBILITY STUDY

Henry A. Miranda, Jr.

Epsilon Laboratories, Inc.
4 Preston Court
Bedford, MA 01730

May 1980

Final Report for period August 1978 through December 1979.

Approved for public release; distribution unlimited.

This research was supported by the Air Force In-House Laboratory Independent Research Fund

Air Force Geophysics Laboratory
Air Force Systems Command
United States Air Force
Hanscom AFB, MA 01731

UNCLASSIFIED

SECURITY CLASSIFICATION OF THIS PAGE (When Data Entered)

REPORT DOCUMENTATION PAGE	READ INSTRUCTIONS BEFORE COMPLETING FORM
1. REPORT NUMBER: AFGL-TR-80-0155	2. GOVT ACCESSION NO.: AD A090 018
3. RECIPIENT'S CATALOG NUMBER:	
4. TITLE (and Subtitle): A MOLECULAR IDENTIFICATION DEVICE FOR INDIVIDUAL SUB-MICRON AEROSOLS: FEASIBILITY STUDY.	5. TYPE OF REPORT & PERIOD COVERED: Final rept.
	6. PERFORMING ORG. REPORT NUMBER:
7. AUTHOR(s): A. Miranda, Jr.	8. CONTRACT OR GRANT NUMBER(s): F19628-78-C-0168
9. PERFORMING ORGANIZATION NAME AND ADDRESS: Epsilon Laboratories, Inc. 4 Preston Court Bedford, MA 01730	10. PROGRAM ELEMENT, PROJECT, TASK AREA & WORK UNIT NUMBERS: 61101F 1L1R8AAA
11. CONTROLLING OFFICE NAME AND ADDRESS: Air Force Geophysics Laboratory Hanscom AFB, MA 01731 Monitor/William K. Vickery/LKD	12. REPORT DATE: May 1980
	13. NUMBER OF PAGES: 35
14. MONITORING AGENCY NAME & ADDRESS (if different from Controlling Office)	15. SECURITY CLASS. (of this report): Unclassified
	15a. DECLASSIFICATION/DOWNGRADING SCHEDULE

16. DISTRIBUTION STATEMENT (of this Report)

Approved for public release; distribution unlimited.

17. DISTRIBUTION STATEMENT (of the abstract entered in Block 20, if different from Report)

18. SUPPLEMENTARY NOTES

This research was supported by the Air Force In-House Laboratory Independent Research Fund

19. KEY WORDS (Continue on reverse side if necessary and identify by block number)

stratosphere, aerosol composition, Mie scattering, laser, flashlamp, spectrograph, balloon-borne system

20. ABSTRACT (Continue on reverse side if necessary and identify by block number)

An experimental feasibility study to demonstrate the viability of a concept for determining the molecular constituency of stratospheric sub-micron particulates on an individual particle basis, is described. Recommendations for continuing the program as far as the demonstration milestone are presented. Included among these are: 1) a means of greatly simplifying the test apparatus set-up (thereby reducing the probability of interruption by critical component failure), and 2) specific investigations to develop engineering data for the design of a future field prototype device.

DD FORM 1 JAN 73 1473 EDITION OF 1 NOV 65 IS OBSOLETE

UNCLASSIFIED

SECURITY CLASSIFICATION OF THIS PAGE (When Data Entered)

TABLE OF CONTENTS

I. INTRODUCTION

This report describes research efforts performed to date under Contract No. F19628-78-C-0168, the ultimate objective of which is the development of a stratospheric balloonborne device for the identification of molecular species make-up of submicron particulates, while simultaneously determining their respective sizes and concentrations on an individual basis. This program was originally intended to demonstrate the overall feasibility of the concept. While this goal has not as yet been achieved for reasons which will be discussed presently, neither has the converse been shown. For this reason, it is recommended that the program be continued.

Many important gaseous minor constituent molecular species resident in the stratosphere, (such as, for example, HNO_3, H_2SO_4, H_2O, HCl, etc.), can exist in the solid or liquid state in the troposphere and stratosphere. The extent to which these constituents can condense and/or evaporate is not known because of several factors, not the least of which is the actual size distribution of the particulates, itself a matter of some recent controversy. It is clear that, whatever the size distribution, the concentration of volatile gaseous material is more than sufficient to support the mass of particulate material known to be resident in the troposphere and stratosphere. Whether significant exchange between the gaseous and particulate state does in fact take place, and more particularly, whether these particles have a role as sources and/or sinks in some form of dynamic equilibrium, is a matter of some speculation. In this regard there is abundant basis in the literature for advancing the role of particulates in the chemistry of volatile constituents.

Moreover, the results of size distribution measurements made with the AFGL/Epsilon sizing spectrometer (Ref. 1) indicate that the total mass of particulate material in the troposphere and the stratosphere appears to be very heavily weighted towards particles less than about 0.35 - 0.40 μm diameter. Should these measurements be proven to be the rule rather than the exception, then the role of particulate exchange with volatile gaseous constituents in the chemistry becomes much more significant than would otherwise be the case. These latter considerations have been an important factor in prompting this development effort.

The basic molecular identification concept involves a sequence of actions which is set in motion once the particle enters a tiny but well-defined sensing zone. This sequence includes: 1) detection of the scattered light pulses from which the sizing information is derived, 2) subsequent measurement of the amplitude of the pulses, 3) illumination of the particle thus detected with 10.6 μm radiation from a pulsed laser to vaporize the material, and 4) illumination with UV light within about 10 microseconds from a suitable pulsed xenon flashlamp to permit subsequent spectroscopic identification of the gaseous material previously vaporized.

The potential for the ultimate success of the concept rests upon certain properties of the various candidate materials, among which are: absorption coefficient at the vaporizing wavelength, vaporization enthalpy, vapor pressure versus temperature, vaporization temperature, excited-state quenching cross-sections, spectroscopic signatures, etc. Some of these properties are well documented for most species of interest, while certain other of the relevent properties for these same species remain largely unknown, especially with regard to spectroscopic information.

Thus it may be necessary to develop the requisite cross-section data for many of the potential candidates. It was our hope to have performed some of these more basic measurements as part of the first year's feasibility demonstration program. Unfortunately, two separate unrelated factors caused the diversion of a significant portion of the contract effort, so that it became impossible to expend any effort along these lines. As a result we were able to investigate only two species, and these in a very restricted manner.

In the next section of this report, a brief description of the planned approach of the device designed to implement this concept, and of the limited results obtained, are presented. Also included are recommendations for continued efforts to advance the work toward the first intended milestone, namely, demonstration of feasibility.

II. DESCRIPTION OF TEST APPARATUS

A. Modification to Existing Sizing Spectrometer

It was recognized at the outset that the cost of designing, fabricating and checking out such a breadboard device might be excessive, owing

to the fact that the concept to be investigated involved the somewhat complicated set of sequential actions mentioned above which had to occur within a short space of time (∿10 microseconds) and within a rather restricted space (∿1/2 mm). Fortunately, Epsilon had at its disposal a balloon-borne aerosol sizing spectrometer which could be modified in a manner that would permit the breadboard demonstration to proceed to completion at a fraction of the above cost while at the same time retaining its original character as a simple particulate sizing spectrometer.

This device (see Ref. 1, 2) consisted of a small bore (1mm diameter) horizontally-oriented sampling inlet tube, which is interrupted within a hermetically enclosed chamber to permit orthogonal illumination by a specially-shaped He-Ne laser beam in the horizontal plane. As the particles transit this sampling tube gap on their way through a similarly-shaped exit tube (fitted with a critical orifice and sampling pump to maintain constant volumetric sampling rate quasiindependent of altitude), they cross the illumination beam. The sensing zone is therefore defined by the sampling airflow diameter and the width of the beam (the latter being about 1/3 mm). The light pulses thus generated are about 60-100 microseconds in duration, and are detected by two annular optical systems operating in forward scattering mode (10° and 30° respectively). A sophisticated electronic processing system performs the pulse height determination, establishes a pulse duration threshold which tracks the DC background level, digitizes the information, and impresses it (together with a host of housekeeping data such as laser power, flow rate, high voltage, altitude, etc.) on to a 9-track magnetic tape in an IBM-360 compatible format for subsequent processing.

The proposed modifications to this device were six fold: 1) insert a second CO_2 pulsed laser module which would place a similarly-shaped high power beam (of 10.6 micron wavelength) so as to be co-linear with the HeNe laser, and which would be fired within 10-20 microseconds after a selectable pulse height threshold was crossed either on the 10° or the 30° channel, or on both channels, 2) insert a xenon flashlamp illumination module which would illuminate a 1 mm diameter area at near-vertical incidence centered on the above-described sensing zone, which could be fired at a

selectable time (within 10-20 microseconds after the laser firing), 3) insert a specially designed slitless spectrometer module utilizing high speed (ASA3000) Polaroid film to record the spectral information for determining the particulate molecular species, 4) make appropriate modifications to the electronic pulse height processing circuitry to permit the necessary logic functions described in 1) and 2) above to proceed, 5) replace the glass beam shaping lens with a barium fluoride lens which (together with an associated pair of optical systems to direct both the HeNe and the CO_2 laser beams comprising part of modification 1) above) would permit both beams to enter the hermetic chamber, and 6) incorporate a specially designed b- le system to reduce unwanted background from the xenon flashlamp to acceptably low levels so as to permit analysis of the spectral information on the photographic plate.

B. Major Components of the Test Apparatus Addition

The three major components of the modification modules, namely 1) the CO_2 laser, 2) the xenon flashlamp, and 3) the slitless spectrograph, are discussed very briefly here.

1) CO_2 Laser

This component, a Gen-Tec Model #DDL2SH, yielded a maximum nominal output of up to 0.5 joule (multimode) in a pulse of about 200-400 nanoseconds duration. (Measurements with an integrating joule-meter indicated that an output of about 0.2 joules/pulse was a more realistically achievable value on a repetitive basis of a pulse every few seconds.) This was shaped so as to provide an illuminating area of 1 mm^2 (or 1.0 x $10^{-2} cm^2$). Taking the lesser value, an output fluence of about 20 joules/cm^2, (which was deemed sufficient to vaporize most particulate materials of interest), was anticipated. At the time that the program was conceived, this was the only pulsed CO_2 laser available which offered promise for subsequent packaging into a balloon-borne configuration. (Others had appeared later, but were more expensive.)

Unbeknownst to us, the laser may have sustained certain very subtle damages in transit which, (according to the manufacturer), could have resulted in its subsequent failure after several thousand pulses. Ordinarily, such a limited-life behavior would have been sufficient to extract

the type of demonstration data consonent with the breadboard nature of the program. However, the problem of coaligning the CO_2 laser beam with the HeNe beam proved to be a much more formidable task than originally contemplated. This unscheduled activity, (which included the surmounting of such problems as dichroic mirrors sustaining irreperable damage by virtue of absorption of the high-power laser beam), used up virtually all the available life of the (deficient) laser. Thus, by the time that alignment was finally achieved, the laser failed. (It was subsequently repaired by the manufacturer and returned to Epsilon just before termination of work, and hence could not be utilized for its intended purpose under the present contract.)

Upon later reconsideration of the coalignment approach (which had been motivated by the original desire to permit rapid disassembly of the modifications and restoration of the system as a sizing spectrometer), it was realized that the rather extensive contract effort devoted to coalignment could have been entirely avoided by two simple incisions elsewhere in the hermetic chamber (which incisions could subsequently have been sealed in a very straightforward manner). Incidentally, this would also have avoided the necessity of modification #5 above.

2) Xenon Flashlamp

This component, a Xenon Corporation Model N-725 linear flashlamp, yielded a nominal output of up to 3 joules per pulse (for a specially-shortened pulse of about 2 microseconds), when energized by an input energy of 20 joules per pulse. The lamp was completely enclosed within a copper tube which performed several functions: 1) provided a ground return path for the electrical energy stored in the capacitor, during the pulse, 2) contained the tube in the event of an explosion, 3) provided an optical enclosure to enhance the temperature (and hence the UV output) during firing, and 4) permitted the mounting of a suitable orifice to define a small circular (3mm diam) source of light near the surface of the linear lamp.

A fraction of the output light exits from this orifice. A lower limit value for this fraction can be derived on the simple assumption that

it is equal to the ratio of the orifice area (about 9 mm^2) to that of the linear dimensions of the luminous region (about 113 mm^2). On this basis then the fraction of output light is equal to or greater than 8×10^{-2}. This is collected by an f/4 optical system, and imaged into a one-millimeter diameter area as mentioned previously. Thus the optical system exhibits a minification factor (m) equal to 3. It can be shown that the solid angle (Ω) subtended by the lens diameter (D) of focal length (f) at the source is given by

$$\Omega = \frac{\pi}{4} \times \frac{D^2}{(1+m)^2 f^2} \quad \ldots\ldots\ldots\ldots\ldots (1)$$

Inserting the appropriate values into the above expression, (namely D/f = 1/4, and m = 3), one obtains $\Omega = 3.1 \times 10^{-3}$ steradian. Thus the total output energy of 3 joules noted above delivers a "useful" output given by $(3/4\pi) \times (8 \times 10^{-2}) \times (3.1 \times 10^{-3}) = 5.9 \times 10^{-5}$ joules. When this energy is delivered over an image area of 1mm diameter the output fluence is then about 7.5×10^{-3} joule/cm^2. This is about 25 times less than the 0.2 j/cm^2 fluence value pertaining to the CO_2 laser illumination.

It should be noted here that the flashlamp used in this program was fabricated from Suprasil, which transmits down to the 1600-1700 Å region. Thus the energy is spread over a fairly broad spectral region extending out to about 2 microns, about 11% of which is between 1900 Å and 2100 Å approximately. This means that a fluence of roughly 8.3×10^{-4} joule/cm^2 is contained in that general region of the spectrum where many molecules can experience photolysis.

Since the xenon illumination focussing optics consisted of a single planoconvex quartz lens, a considerable amount of chromatic aberration was anticipated. This property was used to good advantage by incorporating a focus adjustment into the lens mounting structure. This permitted the illumination system to behave as a spectral filter by the simple expedient of translating the lens along its axis. Our calculations, based upon available dispersion data on quartz, indicated that the spectral bandpass of the filter thus created was about 200 Å FWHM. This was verified by experiment.

With respect to this chromatic property of the illumination lens, a careful series of calibration runs were performed to permit the ready selection of any desired region of the spectrum. These runs were consistent with the theoretical estimates derived from this well known property.

3) Spectrograph

The spectrographic source (i.e., the expanding gaseous vapor) for this system would be illuminated for a very short period of time (i.e., about 2 microsecond duration), commencing at about 10-20 microsecond, after the laser vaporization. Thus it was presumed that the dimensions of the vapor cloud would be in the neighborhood of 100-200 microns diameter during the period of illumination. It was therefore reasoned that a slitless spectrograph would serve well the purposes of the experiment.

This was accordingly designed to view the "point" source from a nearly vertical angle which, for practical reasons of design, was chosen to be in symmetric relation to the illumination optics with respect to a vertical plane including the laser beam. The spectrograph was comprised of the following elements: 1) quartz plano-convex collimating lens, 2) transmission grating (which was transparent down to about 2000 Å, 3) adjustable quartz focussing lens, and 4) Polaroid back housed in a rotatable mount (whose axis of rotation is parallel to the grating rulings). Due to the combined effect of chromatic effects of the quartz lenses and the grating dispersion curve, the focal surface (i.e., the focus of all images of the source as a function of wavelength), lies on a curve that is not readily expressable in a simple analytic fashion. For this reason a focal curve was constructed by means of a series of calculations at discrete wavelengths. The shape of this curve was verified by experiment. A specific angle was empirically selected for the rotatable mount which yielded a reasonably good image from 2000 Å out to the detection limit of the film (about 6500 Å). Moreover the system spatial resolution was found to be comparable with the minimum source dimensions of 100 micron (i.e., 0.1mm).

Having established the fixed angle, it was possible to calibrate the spectrograph in terms of a plate factor (i.e., Å/mm) using a set of Mercury lines and other sources. This was found to be quite linear over the complete range of interest. The plate factor determined in this

manner was 189 Å/mm. It is seen from this that the anticipated minimum source dimension of 0.1 mm would subtend a spectral interval of 18.9 Å. In other words, the spectral resolution of the photographic detection system is about 20 Å nominally, a value which is quite acceptable for the intended analysis (e.g., identification for molecular bands, line radiation, etc.). On an absolute basis, the wavelength uncertainty was determined to be less than ±10 Å, approximately. This was determined by a short series of tests using the edge of the photographic plate as a reference. It was further determined that this latter ingredient was the major source of absolute spectral uncertainty.

These tests were facilitated with the aid of a tiny (0.32 mm diameter) Al_2O_3 "white ball" fabricated especially for this purpose. The ball, (formed by using a small drop of slurry which was then allowed to dry) was carefully placed atop a long thin spindle about 0.1 mm diameter. The latter was fashioned by filing a needle which was then painted with 3M "Black Velvet" prior to affixing the Al_2O_3 ball thereto. This needle was secured to a screw which was in turn mounted onto a plate. A locking nut arrangement permitted the screw to be elevated or lowered in a controlled fashion so as to place the "ball" at the center of the sensing zone. This ball simulated the gaseous vapor source, and served admirably not only for developing the spectrograph plate factor, but also as a means of estimating the system detection threshold (see below).

4) Special Electronic Circuitry

4.1 High voltage pulse circuitry

A xenon flashlamp driving module, purchased from Candela Corporation, Model ED-100U, was utilized. Included as part of this module was a special 0.15 microfarad low-inductance capacitor capable of storing and handling up to 25 joules, and a commercial high voltage power supply, Electro-Optical Instruments, Inc., Integrated laser modulator, Model ILM-70 (for which certain modifications were required). In addition, a mounting fixture and special cylindrical high voltage insulator, together with the copper tube (described previously) and faraday shield, were designed and fabricated as an integral unit.

In this latter connection it should be noted that the possible impact of electromagnetic effects (including inductive as well as radiative

coupling) upon the existing digital circuitry of the aerosol sizing spectrometer was a matter of some concern. In large part, this concern stemmed from the fact that this circuitry (which was not designed with the present application in mind) embodied a rather large network of open unshielded wiring, which comprised a host of antennae across a rather broad region of the spectrum. Therefore considerable attention was accorded to the xenon flashlamp circuitry in an attempt to minimize these effects. As part of this concern, an EGG Xenon flashlamp was procured as a back-up in case this problem had to be mitigated at the source. This lamp suffered the disadvantage of a factor of 2-4 in output, but offered a distinctly offsetting advantage of much greater compactness, which would greatly facilitate shielding measures, should this have proved necessary. Accordingly a duplicate driving circuit was prepared for this component in order to be prepared for this particular eventuality. As things turned out, this was found not required; and the back-up was not used.

On the other hand, it is entirely possible that any such effects that might have been experienced were masked (or rather, preempted) by massive effects of a similar nature generated by the Gen-Tec CO_2 laser. This unit, which constitutes a vastly more serious source of unwanted radiative effects by virtue of: 1) a much higher voltage, 2) much shorter rise times, and 3) virtually total lack of shielding, wrought considerable damage to the digital circuitry of the spectrometer. To illustrate the magnitude of this latter undesirable effect, we note that, on occasion the firing of the laser would cause premature actuation of the xenon flashlamp triggering circuitry output.

4.2 Special logic circuitry

A special circuit was designed to interface with the aerosol sizing spectrometer. It was desired to trigger the CO_2 pulsed laser at a specified time after a particle had been detected, and it was originally hoped that the existing sizing circuitry functions could continue in their normal fashion during the laser and flashlamp firing. However the presence of the aforementioned noise problems quickly forced abandonment of this possibility. Instead it was decided to forego sizing information on the specific particle being vaporized, and resort instead to a statistical assessment of particle size (i.e., from many other particles which were

sized, but not vaporized). Since the purpose of the present program was primarily to demonstrate the basic feasibility of the concept, the relinquishment of such information was of little consequence.

Accordingly the interface circuitry that eventually emerged was one that performed the following functions: 1) established a selectable threshold for both the 10^{o} and the 30^{o} channel output pulse from the sizing spectrometer, 2) generated a trigger pulse to fire either the CO_2 laser, or the xenon flashlamp after a selectable delay, which trigger pulse was itself initiated upon a threshold-crossing from either the 10^{o} channel, or the 30^{o} channel, or both simultaneously, and 3) generate a second pulse that fired the flashlamp after a selectable time following the firing of the CO_2 laser. A complicating feature of the latter function emerged upon discovery that the CO_2 laser itself exhibited a jitter of between 8 and 20 microseconds, approximately.

C. Vaporization and Related Considerations

1) 10.6 micron radiation

Taking 10 kilocalories/mole as a nominal vaporization enthalpy for a typical molecular species, it is useful to state this in terms of the quantity of energy per molecule required for vaporization, and what implications can be inferred from this. Since, from Avogadro's number, $(N) = 6.02 \times 10^{23}$ molecules/mole, then the energy per molecule is simply $10^4/N = 1.7 \times 10^{-20}$ cal/molecule, or 7×10^{-20} joules/molecule. Turning now to the requisite absorption of radiation, it is noted that each photon of 10.6 micron wavelength carries an energy of $hc/\lambda = 1.9 \times 10^{-20}$ joules. Thus the vaporization of a typical molecular species by CO_2 laser radiation would require the absorption of

$$\frac{7 \times 10^{-20}}{1.9 \times 10^{-20}} = 3.7 \text{ photons/molecule, on the average.}$$

This can be stated in terms of the photon fluence in the illumination beam (ϕ photons/cm^2) and the molecular absorption cross section (σ cm^2/ molecule). It is seen on dimensional grounds that

$$\sigma\phi = 3.7 \quad \ldots\ldots\ldots\ldots\ldots\ldots \quad (2).$$

Since the energy fluence of the CO_2 laser beam, (as noted in section B1 above) is 20 joules/cm^2, then the photon fluence is

$$\phi = \frac{20}{1.9 \times 10^{-20}} = 1.05 \times 10^{21} \text{ photons/cm}^2.$$

Thus the required cross section is given by

$$\sigma = \frac{3.7}{1.05 \times 10^{21}} = 3.5 \times 10^{-21} \text{ cm}^2\text{/molecule}.$$

This value can also be expressed in terms of the macroscopic absorption coefficient (k cm^{-1}), where (k) is given by the expression

$$k = \sigma m \quad \ldots\ldots\ldots\ldots\ldots\ldots \quad (3),$$

and where (m) is the molecular concentration (molecules/cm^3). This latter quantity is given by

$$m = \frac{N\rho}{w} \quad \ldots\ldots\ldots\ldots\ldots\ldots \quad (4),$$

where $\rho \equiv$ the density (grams/cm^3)

$w \equiv$ the molecular weight ($\frac{\text{grams}}{\text{mole}}$).

Inserting nominal values for these quantities, namely $\rho = 3$ and $w \approx 70$, one finds

$$m = \frac{6 \times 10^{23} \times 3}{70} = 2.6 \times 10^{22} \frac{\text{molecules}}{\text{cm}^3}.$$

Using this value together with the above cross-section, one finds

$$k = (3.5 \times 10^{-21}) \times (2.6 \times 10^{22}) \approx 91 \text{ cm}^{-1}.$$

This latter value is rather modest, since it implies a mean free path of about 1.1×10^{-2} cm, a value not indicative of heavy absorption. In other words, few materials (of typical density and molecular weight) are sufficiently transparent at this wavelength to avoid vaporization, when illuminated by this beam fluence.

Seen from a slightly different perspective, a spherical particle of diameter (d) absorbs a fraction $1-e^{-kd}$

of the incident radiation along its diameter. Thus a one micron diameter particle (of typical density and molecular weight) will exhibit a (kd) value of (91) x (1×10^{-4}) or 9.1×10^{-3}, and hence the fraction of impinging illumination absorbed will be only

$$1-e^{-0.0091} = 0.91\%.$$

Yet, in spite of this meager absorption, it will be vaporized because of the intense fluence.

In the preceding discussion it has been presumed that vaporization is the only noticeable result of the absorption of sufficient radiation. This is because each photon of 10.6 micron wavelength carries an energy of 1.9×10^{-20} joule, or 0.12ev. Thus its energy is insufficient to break molecular bonds or to cause any significant electronic excitation. The possibility of multiple-photon absorption, which could conceivably give rise to such alternate effects, is not addressed at all, it being considered to be beyond the scope of the intended study.

On the other hand we have kept open minds on this question, recognizing that if such effects were to occur and result in excited states which lead to detectable and identifiable relaxation emission, it would be observed and noted. Should this circumstance come about, appropriate steps would be taken to investigate further along these lines, and the requisite data would be collected if feasible or possible.

2) Xenon Flashlamp Fluence Absorption

2.1 Molecular excitation

It was shown in Section B-2 above that the energy fluence of about 8.3×10^{-4} joule/cm^2 is delivered in the sensing zone in the vicinity of 2000 Å, over a bandpass of about 200 Å. At longer wavelengths the output may be expected to be somewhat lesser (e.g., at 2500 Å and 3000 Å, the fluences are about 3.6×10^{-4} j/cm^2 and 1.7×10^{-4} j/cm^2, respectively, over the same 200 Å bandpass, roughly). At 2000 Å, each photon carries an energy of 1.0×10^{-18} joules, a value considerably greater than that

of the CO_2 laser photons. Hence in terms of the number of photons required per molecule for direct vaporization to occur, (assuming that all the photon energy is dissipated in the form of heat, which of course is an unlikely assumption for several materials of interest), the value in this instance is

$$\frac{7 \times 10^{-20}}{1.0 \times 10^{-18}} = 7.0 \times 10^{-2} \text{ photons/molecule,}$$

on the average. Taking the above energy fluence of 1.2×10^{-3} j/cm^2 applicable to the xenon flashlamp at 2000 Å, one finds the associated photon fluence to be

$$\phi = \frac{8.3 \times 10^{-4}}{1 \times 10^{-18}} = 8.3 \times 10^{14} \text{ photons/cm}^2.$$

Thus the requisite vaporization cross-section is, by recourse to equation (2)

$$\sigma = \frac{7.0 \times 10^{-2}}{8.3 \times 10^{14}} = 8.4 \times 10^{-17} \text{ cm}^2\text{/molecule.}$$

The associated absorption coefficient is, following equations (3) and (4),

$$k = \sigma m = (8.4 \times 10^{-17}) \times (2.6 \times 10^{22}) = 2.2 \times 10^{6} \text{cm}^{-1}.$$

It is seen from these calculations that direct vaporization is much less likely, (though not impossible), in the case of the xenon flashlamp fluence, than in the case of the laser fluence. This is further aggravated by the fact that the rate of delivery of these photons is lower by an additional factor of 10 by virtue of the longer pulse length (i.e., 2 microseconds for the flashlamp as opposed to about 0.2 microseconds for the laser). It should be noted in passing that the chromatic effects (which were viewed as beneficial from an investigative point of view in that it provided a handy filter for examining different regions of the spectrum more or less at will), become a hindrance if one is desirous of using the flashlamp output as a means of vaporization. Thus by simply eliminating chromatic effects it is possible to realize a factor of about 10 improvement in fluence.

On the other hand, other mechanisms beside vaporization are conceivable when the molecules are bathed in UV light. The much more energetic photons (6.25ev in the case of 2000 Å photons) are, for example, capable of breaking molecular bonds, in which case dissociative afterglow becomes a potentially viable detection mechanism. In this connection, since cross-sections for such mechanisms of the order of 10^{-16}-10^{-19} cm^2/molecule are not uncommon, it is very likely conceivable that dissociation would occur directly in the solid state. Whether quenching effects would be small enough to permit the dissociative afterglow to be observed, is questionable. This depends upon the specific quenching cross-sections of the species encountering one another, many of which are unknown. However, on the basis of general knowledge currently extant, this is not thought to be a very likely possibility.

From the foregoing discussion it is obvious that without resort to experiment the question of direct excitation by flashlamp without prior vaporization is likely to remain unclear. As will be seen in the next section, the results of a very limited exploration in this direction will be presented. While these were negative, they were conducted under less than ideal circumstances, so that the results are not necessarily to be viewed as conclusive.

2.2 Xenon flashlamp fluence calibration

An attempt was made to measure the instantaneous xenon flashlamp illumination in the vicinity of the sensing zone by direct means using a calibrated UV-enhanced silicon diode detector. This effort proved fruitless owing to the high frequency noise generated by the flashlamp discharge and associated electronics. Thus in order to avoid expending a disproportionate amount of available contract funds to reduce the noise, it was decided to pursue indirect means, (namely photographic film) for calibration purposes. Though admittedly much less accurate, (i.e., ± a factor of 3-5), such a means is nevertheless adequate for the present purposes.

Accordingly, the white Al_2O_3 ball described above, which had been designed as a wavelength calibration tool, was used for this latter purpose. As will be seen presently, the agreement between

calculated fluence and measured fluence in the sensing zone was found to be quite acceptable. The crude calibration scheme involved the use of Polaroid 668 color film (as well as type 665 print/negative film) as the recording medium, the white ball as a simulant for the particulate material, and a subjective determination of image density levels (in the case of the color film), as well as densitometry measurements (in the case of the type 665 negative). On the basis of these data, together with spectral sensitivity information provided by the manufacturer (in terms of the reciprocal ergs/cm^2 required to yield a stipulated density on the plate versus wavelength), it was possible to derive a value for the fluence.

To do so, it is necessary that the fluence ϕ(joules/cm^2) impinging on the ball be related to the exposure E(ergs/cm^2) on the plate. This relationship is derived as follows:

The radiance R_s (joules/cm^2steradian) emerging from the ball is given by the expression

$$R_s = \frac{\phi A}{4\pi} \quad , \ldots\ldots\ldots\ldots (5)$$

where A ≡ the albedo of the Al_2O_3 material.

The factor (4π) in the denominator expresses the assumption of isotropic scattering from the ball. Invoking the "brightness" theorem, the image irradiance R_I' (joules/cm^2steradian) falling on the photographic film is related to R_s by

$$R_I' = R_s T \quad , \ldots\ldots\ldots\ldots (6)$$

where T ≡ the throughput transmission factor of the entire optical system.

The use of the prime superscript symbol expresses the fact that the energy in the spectral image is dispersed in one dimension on the photographic plate by the action of the transmission grating. Thus an additional factor (g) must be introduced to account for this energy dispersal. Recalling the above plate factor of 189 Å/mm, and taking mean width of the ball to be about 0.2 mm, then the spectral image of the ball on the plate (which would occupy a mean spatial width of about 0.2 mm thereon) occupies a wavelength increment of 189 x 0.2 = 37.8 Å. But since the incident

fluence ϕ is derived from a spectral passband of about 200 Å (recalling the quartz lens chromatic aberration effect described above and its manifestation in terms of a filter), then it follows that the energy associated with the quantity R' would be spread over a rectangular image whose length is $\frac{200}{189}$ = 1.06 mm. Thus

$$g = \frac{0.2}{1.06} = 0.19 \left(= \frac{37.8}{200}\right),$$

and the irradiance of the image (R_I) is less than (R_I') by the factor (g),

$$R_I = R_I' \times g \quad \ldots\ldots\ldots\ldots \quad (7).$$

Combining equations 5, 6 and 7, one obtains

$$R_I = \left(\frac{gTA}{4\pi}\right) \times (\phi) \quad \ldots\ldots\ldots \quad (8).$$

The photographic exposure (E) is related to the irradiance (R_I) by the following expression

$$E = R_I \, \Omega \times 10^7 \quad \ldots\ldots\ldots\ldots \quad (9)$$

where $\Omega \equiv$ the solid angle subtended by the focussing lens at the film plane, and where the factor 10^7 converts joules to ergs. The quantity (Ω) is given by

$$\Omega = \frac{\pi}{4} \left(\frac{1}{f/\#}\right)^2 \quad \ldots\ldots\ldots\ldots \quad (10).$$

Combining equations 8, 9 and 10, one obtains the desired relation

$$\phi = \frac{16(f/\#)^2}{gTA} \times 10^{-7} E \quad \ldots\ldots\ldots \quad (11).$$

The system throughput value (T) was estimated on the basis of the following ingredients: 1) 6 lens surfaces, each transmitting about 95%, 2) a folding mirror transmitting about 80%, 3) a transmission grating transmitting about 60% and with a first order efficiency factor of about 80%. The combined effect of these is to yield a T-value of 0.25. The albedo of the Al_2O_3 is estimated to be about 80%, and the focussing lens

of the spectrograph is f/4. Inserting these values into equation (11) yields the conversion factor

$$\phi = 6.7 \times 10^{-4} E \quad \ldots\ldots\ldots\ldots \quad (12).$$

At an input energy of approximately 20 joules, an image density of about 0.8 was found to have been produced at 3000 Å. From the characteristic curve provided by the manufacturer, the relative exposure corresponding to a density of 0.8 is about 3 times that corresponding to a density of 0.5. The manufacturer indicates that an exposure of about 5×10^{-2} ergs/cm^2 will yield a density of 0.5 at 3500 Å. Though no published data are available below 3500 Å, we have discussed the question of extrapolating the sensitivity down to 3000 Å with knowledgeable personnel at Polaroid, who have advised us that the sensitivity is about the same at this wavelength. Taking this value then, the exposure required in order to yield an image density of 0.8 is about

$$3 \times 5 \times 10^{-2} = 1.5 \times 10^{-1} \text{erg/cm}^2.$$

Since the spectral images were derived from two pulses in each case, the exposure per pulse is

$$E = 1.5 \times 10^{-1}/2 = 7.5 \times 10^{-2} \text{ ergs/cm}^2.$$

Inserting this into equation (12), one obtains

$$\phi = (6.7 \times 10^{-4}) \times (7.5 \times 10^{-2}) = 5.0 \times 10^{-5} \text{ joules/cm}^2.$$

It is recalled from Section C2.1 above that the calculated output fluence of the xenon flashlamp at 3000 Å was estimated to be 1.7×10^{-4} joule/cm^2 per pulse for an input electrical energy of 20 joules. This is only 3.4 times greater than the value derived from the "calibration" scheme described here. In view of the many separate and unrelated factors entering into both numbers, it is considered that the agreement between these is quite good, (and certainly adequate for breadboard test purposes). Viewed from this perspective, it was not thought useful to expend additional contract effort to refine the xenon fluence calibration any further at this time.

One general conclusion can be drawn from the foregoing exercise that we feel may be worthy of note. It is reassuring to know that theoretical estimates of flashlamp fluence are accurate to well within an order of magnitude. This means that in any future design activity relating to specific field instrument parameters involving flashlamps and associated optical components wherein fluence estimates are an important ingredient, one can rely upon a-priori calculations.

III. CONCLUSIONS

A. Experimental Results

As explained previously, the opportunity to vaporize particulates with the CO_2 laser and then at a subsequent point in time subject the gaseous particles to a spectrally controlled xenon flashlamp fluence, which sequence comprised the heart of the proposed concept, was not realized. Since the flashlamp apparatus was ready and available an attempt was made to use this as a backup investigative tool.

An effort was accordingly expended to generate micron (and also submicron) particles of several different materials which offered some promise in terms of demonstration potential. Among these were ammonium sulfate, sodium chloride, silver nitrate, cupric chloride, manganese nitrate, mercuric chloride, hydrogen peroxide and nitric acid. During the course of this work a considerable amount of expertise was gained in the area of controlled particulate generation of specific materials. In this latter connection, the generation of H_2O_2 and HNO_3 provided special challenges owing to their high volatility at room temperatures.

Particle generation was achieved for all the above materials (albeit not without some difficulty) which exist in the solid state at room temperatures. In this regard a Thermo Systems Inc. particle generator, (which employs the principle of hypersonic break-up of a liquid stream) was found indispensible. After a considerable trial-and-error period wherein the virtue of extreme cleanliness was learned (as well as the not insignificant practical arts associated therewith), the use of such a device became more or less routine.

These materials were selected because they were: 1) readily available in sufficient purity, 2) easy to work with, 3) exhibited molecular binding

energies (of the major radicals) whose values were low enough to be consistent with the hypothesis of potential photolysis, 4) exhibited reasonably low volatilization temperatures thereby increasing the possibility of vaporization, and 5) comprised major radicals which offered the potential of detection by afterglow radiation.

In several instances some apparent spectral signatures were observed. In all cases, however, efforts to rule out other possible origins of such spectral signatures yielded unmistakeable evidence that the earlier results had been illusory.

Finally, an effort to generate both H_2O_2 and HNO_3 was initiated. Both of these materials were excellent candidates for this study because: 1) their presence in the stratosphere is well established, 2) they may play an important role in the chemical physics of particulate/gaseous exchange (especially in the case of HNO_3), and 3) adequate data are available in the open literature on which to base experiments. On the other hand, both of these materials are much more difficult to handle for several reasons. For example, it was found unfeasible to utilize the TSI instrument because: 1) in the case of HNO_3, the tiny, calibrated aluminum orifice (which is a most important component of this device) would have been destroyed, and 2) operation at the requisite low temperatures would have necessitated yet another major learning effort. For these reasons it was decided to forego the niceties of uniform sizes (a unique advantage of the TSI instrument), and accept much wider (and unspecified) distribution of sizes which results when one uses a conventional nebulizer operating on the Bernoulli principle.

We were able to generate copious quantities of both these latter materials in particulate form. However, it was not possible to deliver the H_2O_2 particulates into the test apparatus because of premature evaporation in the delivery flow system. Therefore the pursuit of this attractive demonstration material was abandoned for the time being in favor of HNO_3. This latter attempt proved successful. A few preliminary test runs were conducted with HNO_3 particulates during the rather limited time available. No spectral identification data have as yet been obtained.

B. Discussion

The total absence of positive results for xenon flashlamp illumination was somewhat surprising in view of the fact that published photolysis cross-section and afterglow data for both H_2O_2 and HNO_3 (Ref. 3,4) indicated that, apart from quenching effects, positive results should have been observed. Thus, on the basis of the confidence we have in the validity of our calculations (which we believe was amply demonstrated in Section II above), we can only conclude that some form of quenching must have been taking place. It is also possible that the lack of complete vaporization may have played a major role in reducing the emission by mechansims other than the resonance radiation under consideration here. In support of this contention two separate calculations are presented for both H_2O_2 and HNO_3 particulates. Two different mechanisms are considered, one being applied to each of the two materials.

1 - H_2O_2 Calculations (one-step mechanism example)

The energy fluence at 2000 Å is $(\phi) = 8.3 \times 10^{-4}$ joules/cm^2 (see Section C2.1 above), and the photon fluence is $(\phi_p) 8.3 \times 10^{14}$ photons/cm^2. The reaction of interest here is the photolysis of hydrogen peroxide by photons in the wavelength region of 2000 Å, as characterized by:

$$H_2O_2 + h\nu \longrightarrow OH + OH \quad \ldots\ldots\ldots\ldots \quad (13).$$

The mean cross-section for this reaction is $(\sigma) = 1 \times 10^{-18}$ cm^2/molecules (or greater) in the 200 Å interval centered at 2000 Å. The number of reactions per particle (N_R) is given by

$$N_R = \phi_p \sigma m V \quad \ldots\ldots\ldots\ldots\ldots \quad (14)$$

where m ≡ the molecular concentration $\left(\frac{\text{molecules}}{\text{cm}^3}\right)$

V ≡ volume occupied by the particle.

Expressing the volume in terms of the (spherical) particle diameter (d), it follows that

$$N_R = \frac{4}{3} \pi \phi_p \sigma m d^3 \quad \ldots\ldots\ldots\ldots \quad (15).$$

The excitation of the OH radical to the $A^2\Sigma^+$ excited state is presumed to occur upon the breaking of the bond. Subsequently, if the radical is undisturbed (e.g., by quenching), it will decay to the $X^2\pi$ ground state within a period of 1 - 1.2 microsecond (Ref. 5,6). The resonance (0,0) transition yields a "linelike" (i.e., relatively narrow) band of about 56 Å centered at 3090 Å.

An alternative mechanism for excitation is: 1) vaporization, followed by 2) photolysis with simultaneous excitation of OH $A^2\Sigma^+$ as above. This is also investigated in the next subsection (using HNO_3 as the example material). Assuming for the moment that each reaction results in one excited OH radical which subsequently relaxes by the emission of one photon, then the number of photons emitted (N_p) is equal to (N_R). The source fluence per unit solid angle (ϕ_S'), assuming isotropic emission, is given by

$$\Phi_S' = \frac{Np/4\pi}{\pi D^2/4}$$

$$= \frac{4}{3\pi}\,\phi_p \sigma m(d)^3 \frac{1}{D^2} \quad \ldots\ldots\ldots \quad (16)$$

where D is the diameter of a resolution element of the imaging system.

The image photon exposure E_p is given by

$$E_p = \phi_S' \Omega T_I \left(\frac{\text{Photons}}{cm^2}\right) \quad \ldots\ldots\ldots\ldots \quad (17)$$

where Ω is taken from equation (10), and T_I is the throughput of the spectrograph optics.

The value of (T_I) differs slightly from the value of (T) used in equation (8), in that the losses in the xenon flashlamp transmitting optics are deleted. Hence $T_I = 0.32$, and

$$E_p = \phi_S' \frac{\pi}{4} \left(\frac{1}{f/\#}\right)^2 \times 0.32 = \phi_S' \frac{0.32\pi}{64} = 0.0157\,\phi_S' \quad \ldots \quad (18),$$

and since the number of (OH)* relaxation photons/erg = 1.6×10^{11}, (λ being 3090 Å) the image exposure (E_I) is simply

$$E_I = E_p/1.6 \times 10^{11} = 1.0 \times 10^{-13} \phi_S' \ (erg/cm^2) \quad . \quad . \quad (19).$$

Substituting for ϕ_S' from equation (16),

$$E_I = 1.0 \times 10^{-13} \times \frac{4}{3\pi} \phi_p \sigma m (d)^3 (\frac{1}{D^2})$$

$$= 4.3 \times 10^{-14} \phi_p \sigma m (d)^3 \frac{1}{D^2} \quad . \quad . \quad . \quad . \quad . \quad . \quad . \quad . \quad (20).$$

For H_2O_2, the molecular concentration (m) is 3.3×10^{22} molecules/cm^3. Taking a nominal 1-micron diameter, (d) is 1×10^{-4} cm; and inserting the values (ϕ_p) = $8.3 \times 10^{14} \frac{photons}{cm^2}$ and (σ) = 1×10^{-18} ($\frac{cm^2}{molecule}$), and D = 1×10^{-2} cm, then

$$E_I = \frac{(4.3 \times 10^{-14}) \ (8.3 \times 10^{14}) \ (1 \times 10^{-18}) \ (3.3 \times 10^{22}) \ (1 \times 10^{-4})^3}{(1 \times 10^{-2})^2}$$

$$= 1.2 \times 10^{-2} erg/cm^2 \quad . \quad . \quad . \quad . \quad . \quad . \quad . \quad . \quad . \quad . \quad . \quad . \quad (21).$$

It is recalled from Section C2.2 above that, according to the manufacturer's data for Polaroid Type 665 film (ASA75), the exposure yielding a density of 0.5 is $5 \times 10^{-2} ergs/cm^2$. However the film used for the actual tests was far more sensitive, namely Polaroid Type 665 (ASA 3000), wherein the detection threshold is about $2 \times 10^{-3} ergs/cm^2$. Comparing this with the value of 1.2×10^{-2} erg/cm^2, it is seen that the experiment has a built-in safety factor of about six for hydrogen peroxide.

2 - HNO_3 Calculations (2-step mechanism example)

In this subsection are presented the anticipated signal levels for nitric acid particulates of one micron diameter, using the alternate scheme mentioned above in order to explore certain of the dynamics of the excitation process, and to provide the reader with a better basis for comparison among the various possibilities. The following physical properties of HNO_3 are noted in tabular form:

molecular weight (w)	: 63
specific heat	: 0.3 cal/gram-degree centigrade (assumed)
density (liquid)	: 1.5 grams/cm^3
vaporization enthalpy	: 9.5 k cal/mole
vaporization temperature	: 293° K(+20°C)
temperature of particles injected into system	: +3°C
Total energy required for vaporization	: 460 cal/cm^3 (calculated from above) (= 6.3×10^{-20} joules/molecule)
Energy required to raise temperature to vaporization temperature	: 2×10^{-22} joules/molecule.

The UV absorption of HNO_3 has been investigated by others (Ref. 7,8), so that the absorption cross-sections are fairly well known: For example, at 1900 Å, 2000 Å, and 2100 Å, the values are 15×10^{-18}, 6×10^{-18} and 1×10^{-18} cm^2/molecule, respectively. Recalling that the energy fluence (ϕ) in the sensing zone is 8.3×10^{-4} joule/cm^2, and taking an average σ-value of 5×10^{-18} over this passband, one finds that the total energy absorbed between 1900 and 2100 Å is

$$(\sigma) \times (\phi) = 8.3 \times 10^{-4} \times 5 \times 10^{-18} = 4.2 \times 10^{-21} \text{ joule/molecule} \quad . \quad . \quad (22).$$

From the tabular data above, the energy required to raise the temperature to the vaporization temperature is 2×10^{-22} joule/molecule. Thus about 95% of the energy absorbed is available for vaporization, since presumably all the molecules will have been raised through the requisite 20°C interval to the vaporization point. It is therefore not unreasonable to assume that the remaining energy is in fact used up in vaporization of a fraction of the molecules. On this assumption the fraction vaporized is given by the ratio

$$\frac{\text{energy available/molecule}}{\text{energy required /molecule}} = \frac{(.95) \times (4.2 \times 10^{-21})}{6.3 \times 10^{-20}} = 6.3\% \quad . \quad . \quad . \quad (23).$$

A 10% solution by volume of HNO_3 in H_2O was used. The molecular concentration of HNO_3 (m_n) = 1.4×10^{22}, while that of water (m_w) is 3.3×10^{22} $\frac{\text{molecules}}{cm^3}$.

Therefore the molecular concentration of the mixture ($\bar{m}$) = 0.9 x 1.4 x 10^{22} + 0.1 x 3.3 x 10^{22} = 1.6 x 10^{22} molecules/cm^3. Since the absorption cross-section for water in the vicinity of 2000 Å is negligibly small as compared to that of HNO_3, the important parameter of interest here is not ($\bar{m}$) but rather (m_n), which is 0.1 x 3.3 x 10^{22} = 3.3 x 10^{21} molecules/cm^3. With the above information in hand, it is possible to estimate the spectral image exposure E_I from equation (20). Given that only 6.3% of these are vaporized, then the molecular concentration of interest here (i.e., the appropriate value of (m) to be inserted in this equation) is

$$m = (6.3 \times 10^{-2}) \times (3.3 \times 10^{21}) = 2.1 \times 10^{20} \text{ molecules/cm}^3 \quad . \; . \; (24).$$

As the molecules expand upon having been vaporized, they encounter illumination photons that are adjacent (both spatially and spectrally) to those used up in the initial absorption. Let us assume that the total fluence of new photons to which these gaseous molecules are exposed is about 50% of the original value. Then

$$\phi_p = \frac{0.5 \times 8.3 \times 10^{-4}}{1 \times 10^{-18}} = 4.2 \times 10^{14} \frac{\text{photons}}{\text{cm}^2} \quad . \; . \; . \; . \; . \; . \; . \; . \; (25).$$

The photolysis cross-section (σ) is identical to that employed for vaporization, namely 5 x 10^{-18}. Retaining the particle diameter (d) = 1.0 x 10^{-4} cm and the image resolution diameter (D) = 1.0 x 10^{-2} cm (as in the case of H_2O_2, and inserting these into equation (20), one obtains

$$E_I = \frac{(4.3\text{x}10^{-14})(4.2\text{x}10^{14})(5\text{x}10^{-18})(2.1\text{x}10^{20})(1\text{x}10^{-4})^3}{(1 \times 10^{-2})^2} = 1.9\text{x}10^{-4} \text{ erg/cm}^2 \; . \; (26).$$

This value is about one order of magnitude smaller than the 2 x 10^{-3} erg/cm^2 detection threshold level for the high speed film used. Thus if one were to integrate for 10 shots, the threshold level would just be reached.

Since up to 16 shots were used without observing the slightest trace of any observable spectral signatures, it would appear that direct excitation is not the dominant excitation mode. Actually however, neither this, nor the one-step mechanism can be ruled out, because in any event gaseous collision quenching of OH excited states drastically reduces the observable resonance radiation, as can be seen from the following.

3. Quenching

It is shown in Reference 6 that the fraction (Q) of excited A-state molecules returning to the ground x-state by radiation, is given by

$$Q = \frac{K_r}{K_r + K(N_2)\left[N_2\right] + K(O_2)\left[O_2\right]} \quad \ldots\ldots\ldots\ldots\ldots (27)$$

where $K(N_2) \equiv$ bimolecular quenching rate constant of the A-state by Nitrogen molecules

$K(O_2) \equiv$ bimolecular quenching rate constant of the A-state by Oxygen molecules

$\left[N_2\right] \equiv$ concentration of nitrogen molecules

$\left[O_2\right] \equiv$ concentration of oxygen molecules

$K_r \equiv$ the A-state radiative rate

Inserting the values listed below into equation 27,

$$K_r = 1.2 \times 10^6/\text{sec}$$

$$K(N_2) = 2.0 \times 10^{-11}\ \text{cm}^3/\text{sec} \qquad \left[N_2\right] = 2.0 \times 10^{19}\ \text{molecules/cm}^3$$

$$K(O_2) = 6.0 \times 10^{-11}\ \text{cm}^3/\text{sec} \qquad \left[O_2\right] = 5.4 \times 10^{18}\ \text{molecules/cm}^3$$

One obtains $Q = 1.6 \times 10^{-3}$. In actuality the oxygen concentration was zero during the tests (because pure N_2 was used in the nebulizing flow. This results in a Q-value of 3.2×10^{-3}. In other words quenching drastically reduces the OH 3090 Å resonance radiation emission.

A final note with respect to quenching should be made here. From the foregoing analysis, it is clear in retrospect that quenching effects were severe enough to have masked alternate attenuation mechanisms that might have otherwise been identified by the tests run to date. In this connection we wish to point out that the use of the CO_2 laser, wherein the energy is deposited in a duration about 200 nanoseconds (which is 1/10 that of the xenon flashlamp), would more closely approximate explosive volatilization. In this event there is a far better opportunity of develop-

ing a "snowplow" effect in the surrounding atmospheric molecules, whereby they are "swept out" by this action, and thus not be available for quenching, (especially with regard to resonance transitions).

4 - *Snowplowing*

The plausibility of snowplowing is supported by the heuristic argument that the snowplow effect will persist out to a radius wherein the expansion momentum equals the total random momentum of all atmospheric molecules contained therein. This diameter can be determined in the following manner: A material expanding initially with a radially-directed speed (v_v) will become essentially randomized (at which point the material will have arrived at diffusive equilibrium with the surrounding ambient air molecules), when these molecules have reached the periphery of a sphere whose diameter (d_L) is given

$$\frac{d_L}{d_v} = \left(\frac{m_v}{m_L}\frac{v_v}{v_L}\frac{m}{L}\right)^{1/3} \quad \ldots\ldots\ldots\ldots\ldots\ldots (28)$$

where $m_v \equiv$ mass of each particulate molecule

$m_L \equiv$ mass of each ambient air molecule

$v_v \equiv$ initial radial speed of the particulate molecules

$v_L \equiv$ average speed of the ambient air molecules

$L \equiv$ the Loschmidt number (2.7×10^{19} molecules/cm^3)

$d_v \equiv$ the diameter of the particle vaporized

$m \equiv$ molecular concentration of the particulate material (2.6×10^{22} molecules/cm^3)

Assuming a typical vaporization temperature of, say, 200°C, then

$v_v/v_K = (\frac{473}{273})^2 = 3.0$, and taking the typical molecular weight of 63,

then $m_v/n_L = \frac{63}{29} = 2.2$. Inserting the appropriate values into equation (28), one obtains $d_L = d_v \left(3 \times 2.2 \times \frac{2.7 \times 10^{22}}{2.6 \times 10^{19}}\right)^{1/3} = 18\, d_v$ . . . . (29).

Because of the cube root relation of equation (29) it is seen that the ratio d_L/d_v is not very sensitive to the factors derived from temperature and mass ratios. From the point in time at which snowplowing ceases, diffusive processes take over which redistribute the ambient molecules within the spherical volume. During this period (which persists for several microseconds typically), it can safely be presumed that quenching effects will not be operative.

C. Recommendations

On the basis of the experimental evidence together with the supportive calculational effort as described in the preceding sections of this report relating to spectral stimulation of the particulate molecular species, several conclusions can be drawn which we believe are useful for future planning purposes. However, before setting these forth it would be helpful to review the ingredients of the concept and to summarize the major milestone of the accompanying activity. Hopefully, this exercise will serve to establish a better perspective from which to evaluate the progress made to date, and thereby to increase the probability of future success.

We begin by reiterating the basic concept, namely 1) vaporization of the solid/liquid particle, followed by 2) illumination with a source and 3) spectral identification of the material. It is also recalled that the initial phase of the present program involved a demonstration of the viability of this concept, an objective which has not as yet been achieved. Vaporization, by the use of a separate module, namely the pulsed CO_2 laser, (which would necessarily inject complexity into the ultimate hardware), was viewed from the outset as having two-fold merit: 1) an insurance measure against failure, and 2) a separate (and very useful) investigative tool to further explore the rather significant body of information relating to this project which presently remains unknown, (such as for example, various types of reaction cross-sections versus wavelength, etc.). Early calculations of a cruder character than presented here had substantiated

that vaporization could also be achieved by flashlamp illumination, (albeit with a somewhat lesser margin of safety); and its potential as a back-up for this purpose had been stated previously. On the other hand (as might be suspected), the use of a xenon flashlamp as a tool for vaporization is in sharp conflict with its use as a spectral illumination tool. The conflict manifests itself primarily in terms of the selection of the optical parameters of the system.

One such conflict has already come to light in the previous discussion (see Section C2.1 above). As stated there, the chromatic effects, which were desirable from the standpoint of its use as a spectral source, become seriously detrimental (by a factor of as much as 10) from the standpoint of its use as a vaporization tool. Another conflict arises from the necessity of suppressing unwanted background in the spectromatic detection system. This is greatly facilitated by the use of a narrow pencil of illumination beam, which necessarily involves low-speed illumination optics (in this case, f/4), whereas if one were to use the flashlamp for vaporization, a much faster system could be employed (e.g., f/0.8 or so, thereby realizing an additional factor of about 25).

Therefore, the negative results obtained with the xenon flashlamp are not necessarily an indication that vaporization is unfeasible, but rather as an indication that, if and when this approach is attempted again, efforts must be implemented to maximize the vaporization fluence therefrom. Incidentally, it follows from the inherently conflicting optical parameter requirements, that two separate flashlamp systems will be necessary: one for vaporization, and second, (fired after an appropriate delay to permit internal fluorescence decay phenomena to relax, etc.) for spectral illumination.

From the foregoing discussion, one recommendation is seen to emerge, namely that some thought should be given early in the breadboard phase of any follow-on program, to the incorporation of a special vaporization module as a substitute for the laser module. This again is viewed as an insurance measure but pointing in this case towards the final design of a working prototype field unit. This latter concern is a separate matter issuing from our experience with radiative effects associated with the

specific laser hardware presently in hand, (see Section B4.1 above). Whether this is a common trait of all such laser systems currently available in the marketplace, or is a deficiency unique to the Gen-Tec design, cannot be established in advance. Therefore, we believe it a matter of prudence to give some consideration to back-up measures in this eventuality.

That vaporization appears to be necessary is supported by the fact that direct excitation yielded negative results in all cases. In this regard, however, the negative results were not at all surprising, owing to the fact that spectral excitation of species in the solid/liquid state is quite improbable. This is due to the host of competing radiationless relaxative transitions for excited electrons by virtue of the close proximity of neighboring molecules. On the other hand, there is a remote possibility that Raman spectra might be observable by direct laser illumination. This should be kept in mind since if feasible, it would obviate the need for vaporization altogether, (and at the same time eliminate the present requirement for two sequential pulse firings).

The problem of excited state quenching from collisions with ambient gaseous molecules needs to be given further attention. The contention that "snowplowing" provides a region of space (and a segment of time) devoid of quenching, is an important ingredient; and a corrolary question relating thereto, is whether the much shorter duration available with laser excitation is necessary to support snowplowing, or whether snowplowing will prevail in any case with the more prolonged flashlamp illumination. If possible, tests should be devised to provide an answer to this question. (It should be noted that this question also is motivated by considerations having to do with detailed design of the final working prototype unit, and as such does not relate directly to the breadboard demonstration effort.)

The possibility of direct excitation and/or ionization of molecular species by the CO_2 laser concomitantly with vaporization (through the mechanism of multiple photon absorption) should be kept in mind. As shown in Section C1 above, a typical material would require the absorption of only 3.7 photons per molecule on the average, in order to achieve

vaporization. This is not a very large number from the standpoint of multiple-photon effects. On the other hand, the absorption of such a small number of photons per molecule is associated with a rather small absorption, (as evidenced by the 91-cm mean free path noted in the text). Many materials exhibit much higher absorption than the minimum required for vaporization. Since the number of photons per molecule increases in direct proportion to the absorption cross-section (or inversely as the mean free path), the probability of multiple photon events is accordingly increased. For example, it is not unlikely that a material should be encountered with a mean free path of about 0.1 mm. In this case the number of photons per molecule would be 37,000. Since these are absorbed within a period of 200 nanoseconds, the possibility of several photons being absorbed before significant relaxation occurs, cannot be altogether ruled out.

Taking all of the above factors into account, we are convinced of the present potential for success. Indeed the efforts expended on the present program have reinforced the original conclusions which motivated the investigation. Thus, despite the results achieved to date, we believe the overall technical concept remains valid. The failure of the CO_2 laser was a crucial factor in this regard, a factor whose importance was not fully appreciated at the time. The supporting calculations which were presented in the previous section have been useful in elucidating the role of various mechanisms (e.g., vaporization, quenching, snowplowing) as well as differentiating between two distinct uses of the flashlamp, etc. For these reasons it is recommended that the program be continued to the completion of the feasibility demonstration phase. As has been amply shown above, the CO_2 laser is an integral part of this activity. However, we strongly recommend that attempts to introduce the laser beam coaligned with the HeNe laser beam be abandoned, and that it be inserted into the sampling chamber in a manner that is far less complicated.

Some attention should also be given to the matter of introducing candidate species into the system. In this connection it would be beneficial to incorporate a means of introducing different gases into the

nebulizing apparatus. This would facilitate the exploration of quenching effects as part of the prototype design phase (assuming the success of the demonstration phase).

Finally, the use of absorption spectra for the identification of selected gaseous molecular species, (a possibility of which we were aware at the outset but failed to mention explicitly because of its obvious potential), should be considered. This can be readily implemented by relatively minor modifications to the flashlamp illumination module. The exploration of this potentially useful spectroscopic mechanism,—especially for those transitions involving excitation from ground-state (i.e., resonance) transitions — had been planned as part of the present program effort, and hopefully may be considered in the future.

IV. REFERENCES

Ref. 1: "Balloon Measurements of Stratospheric Aerosol Size Distribution Following a Volcanic Dust Incursion", H. A. Miranda, Jr., & J. Dulchinos AFCRL-TR-75-0518, Final Report, Contract F19628-75-C-0004, Aug. 1975 (52 pages)

Ref. 2: "Improvements and Modifications to the Epsilon/AFGL Balloonborne Submicron Particle Counter", H. A. Miranda, Jr., and J. Dulchinos, AFGL-TR-76-0211, Final Report, Contract F19628-76-C-0104, Sept. 1976, (15 pages).

Ref. 3: L. T. Molina, et. al., Geophys. Res. Lett., 4, 58 (1977).

Ref. 4: H. S. Johnston, et. al., J. Phys. Chem., 78, 1 (1974)

Ref. 5: T. Carrington, J. Chem. Phys. 41, 2012 (1964).

Ref. 6: J. G. Anderson, Geophys. Res. Lett., 3, 165 (1976).

Ref. 7: H. S. Johnston, et. al., J. Phys. Chem., 78, 1 (1974).

Ref. 8: H. S. Johnston, R. Graham, J. Phys. Chem. 77, 62 (1973).